# On Achievable Rates of MIMO Systems with Nonlinear Receivers

Georgios K. Psaltopoulos, Florian Troesch and Armin Wittneben
Communication Technology Laboratory, ETH Zurich, CH-8092 Zurich, Switzerland
Email: {psaltopoulos, troeschf, wittneben}@nari.ee.ethz.ch

***Abstract*— *Multiple input multiple output* (MIMO) communication systems are popular for achieving high rates, but at the same time they suffer from high implementation cost. Hence, their adoption to future distributed systems, e.g., sensor networks, is stalled due to the stringent cost and power constraints of the node design. One solution is the combination of MIMO systems with nonlinear detectors, i.e., amplitude or phase detectors, which are known for their cheap implementation cost and low power consumption. We provide semi-analytical results for achievable rates in MIMO systems that use nonlinear detectors for the fast fading channel, as well as outage probabilities for the same detectors in the slow fading case.**

## I. Introduction

*Multiple input multiple output* (MIMO) systems have been a hot research topic for over a decade now. Results on the capacity of MIMO systems [1], [2] revealed that high rate gains are possible at high *signal-to-noise ratios* (SNRs) as compared to *single input single output* (SISO) systems. These gains are achieved through spatial multiplexing. However, MIMO systems studied so far employ *linear detectors*, either coherent, which perform carrier phase recovery and channel estimation, or non-coherent ones. We refer to linear detectors under the notion that both the real and imaginary part of the complex-valued received signal are retrieved by the receiver. Nevertheless, linear detection requires expensive circuitry, e.g., linear amplifiers, and high power consumption, e.g., frequency synthesis, even for SISO systems. In MIMO implementations, where multiple receiver chains are required, the total cost rises even more. This could be a critical problem in applications like sensor networks, which rely on low-cost and/or low-power nodes. As illustrated in [3], the increased circuit energy consumption dominates the total power consumption for short-range transmission. Thus, the adaptation of MIMO systems to such scenarios requires low-cost alternatives.

To this end, *nonlinear detection*, i.e., amplitude or phase detection, is known as a low-cost approach to receiver design in SISO systems. These nonlinear techniques extract either the amplitude or the phase of the received signal and can be implemented with simple circuitry. Amplitude detectors can be realized with a diode and a low-pass filter, avoiding the power consuming frequency synthesis. Phase detection on the other side avoids the expensive linear amplifiers by using cheap amplifiers, e.g., clipping amplifiers, since the amplitude of the received signal bears no information.

Combining multiple antennas with nonlinear detectors seems to be a promising technique for future low-cost distributed systems. We assume that the receiver has perfect *channel state information* (CSI). There are different ways a nonlinear detector can gain CSI. It was shown in [4] that channel estimation is possible for phase detection, where the fading channel gains are estimated from the variance of phase samples. In a time division duplex system, where the uplink and downlink channel is the same, we can assume that an access point estimates the channel and signals it back to the individual nonlinear nodes. In the case of amplitude detection, channel knowledge is sufficient up to a phase shift.

So far, the capacity of phase modulation has been investigated in [5] for SISO systems only. The capacity for MIMO systems using nonlinear receivers is not yet known. In our work we provide semi-analytical results for *achievable rates* of MIMO systems with nonlinear detection in fast fading channels. Furthermore, simulation results show that nonlinear detectors achieve full diversity in slow fading channels. In Section II, we describe the system model and the reference system we use for comparison. In Section III, we derive the mutual information expression which we will evaluate numerically. Section IV describes the numerical technique we use and the simulation results in Section V reveal that nonlinear techniques benefit from the use of multiple antennas at transmitter and receiver in a similar way as the linear techniques.

Throughout the paper, bold lower and upper case letters stand for random vectors and matrices, respectively. $\mathrm{E}[\bullet]$, $\mathrm{I}(\bullet)$, $\mathrm{h}(\bullet)$ and $\mathrm{p}(\bullet)$ denote expectation, mutual information, differential entropy and probability density, respectively. $\boldsymbol{A}_{ij}$ is the $(i,j)$-th element of matrix $\boldsymbol{A}$ and $(\bullet)^{\mathrm{H}}$ denotes complex-conjugate transposition.

## II. System Model and Linear Capacity

We consider a MIMO system with $N_{\mathrm{T}}$ transmit and $N_{\mathrm{R}}$ receive antennas. The system model is depicted in Fig. 1. The transmitter sends the signal vector $\boldsymbol{s} \in \mathbb{C}^{N_{\mathrm{T}}}$ over the memoryless flat fading channel $\boldsymbol{H} \in \mathbb{C}^{N_{\mathrm{R}} \times N_{\mathrm{T}}}$, with tap-gain $\boldsymbol{H}_{ij}$ from the $j$-th transmit to the $i$-th receive antenna. The received vector $\boldsymbol{x} \in \mathbb{C}^{N_{\mathrm{T}}}$ is perturbed by a zero-mean circularly symmetric Gaussian noise vector $\boldsymbol{w} \in \mathbb{C}^{N_{\mathrm{R}}}$, with autocorrelation function $\mathrm{E}[\boldsymbol{w}_k \boldsymbol{w}_l^{\mathrm{H}}] = \sigma_w^2 \boldsymbol{I}_{N_{\mathrm{R}}} \delta(k-l)$, where $k$ and $l$ are time instants. A nonlinear detector operates elementwise on the perturbed vector $\boldsymbol{r}$ and extracts either the amplitude or the phase of the complex signal. The real observed vector $\boldsymbol{y} = g(\boldsymbol{r}) \in \mathbb{R}^{N_{\mathrm{R}}}$, $g : \mathbb{C}^{N_{\mathrm{R}}} \mapsto \mathbb{R}^{N_{\mathrm{R}}}$, misses

1-4244-1429-6/07/$25.00 ©2007 IEEE

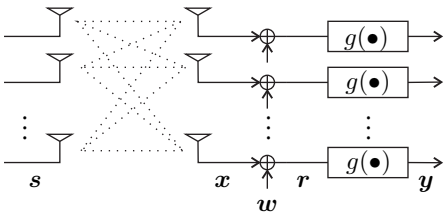


Fig. 1. MIMO System Reference Model

one dimension of the two-dimensional (complex) transmitted signal. The receiver has perfect knowledge of the channel matrix realization $\boldsymbol{H}$ at any time.

When $g(\boldsymbol{r}) = \boldsymbol{r}$, we obtain the linear reference system. The received vector is then given by

$$\boldsymbol{y} = \boldsymbol{H}\boldsymbol{s} + \boldsymbol{w} \tag{1}$$

and the capacity with a total transmit power constraint $P$ and perfect receive CSI has been characterized in [1], [2]. For a stationary memoryless channel, the ergodic capacity is given by

$$C_{\text{lin}} = \mathrm{E}_{\boldsymbol{H}}\left[\log\det\left(\boldsymbol{I}_{N_{\mathrm{R}}} + \frac{\mathrm{SNR}}{N_{\mathrm{T}}}\boldsymbol{H}\boldsymbol{H}^{\mathrm{H}}\right)\right], \tag{2}$$

and the capacity achieving input distribution for i.i.d. Rayleigh fading is circularly symmetric complex Gaussian, $\boldsymbol{s} \sim \mathcal{CN}(\boldsymbol{0}, \sigma_s^2\boldsymbol{I}_{N_{\mathrm{T}}})$. The average SNR per receive antenna is defined as

$$\mathrm{SNR} = \frac{P}{\sigma_w^2} = \frac{N_{\mathrm{T}}\sigma_s^2}{\sigma_w^2}. \tag{3}$$

For high SNR values, the capacity is approximately given by

$$C_{\text{lin}} \simeq N_{\min}\log\frac{\mathrm{SNR}}{N_{\mathrm{T}}} + \sum_{i=1}^{N_{\min}}\mathrm{E}\left[\log\lambda_i^2\right], \tag{4}$$

where $N_{\min} = \min(N_{\mathrm{T}}, N_{\mathrm{R}})$ and $\lambda_i$'s are the singular values of $\boldsymbol{H}$. Thus, the slope of the capacity curve is proportional to the degrees of freedom $N_{\min}$ of the MIMO channel [6].

## III. Rate Computation

Since we assumed that the channel $\boldsymbol{H}$ is memoryless, the capacity is given by the maximum mutual information between the channel input $\boldsymbol{s}$ and the detector output $\boldsymbol{y}$. Furthermore, since $\boldsymbol{H}$ is known to the receiver, the channel output is the pair $(\boldsymbol{y}, \boldsymbol{H})$. The mutual information can be written as

$$\mathrm{I}(\boldsymbol{s}; \boldsymbol{y}, \boldsymbol{H}) \;=\; \mathrm{E}_{\boldsymbol{H}}[\mathrm{I}(\boldsymbol{s}; \boldsymbol{y}|\boldsymbol{H} = H)], \tag{5}$$

since $\boldsymbol{s}$ and $\boldsymbol{H}$ are statistically independent. From the chain rule for mutual information, we have

$$\mathrm{I}(\boldsymbol{s}, \boldsymbol{x}; \boldsymbol{y}|\boldsymbol{H}{=}H) = \mathrm{I}(\boldsymbol{x}; \boldsymbol{y}|\boldsymbol{H}{=}H) + \mathrm{I}(\boldsymbol{s}; \boldsymbol{y}|\boldsymbol{x}, \boldsymbol{H}{=}H), \tag{6}$$

$$\mathrm{I}(\boldsymbol{s}, \boldsymbol{x}; \boldsymbol{y}|\boldsymbol{H}{=}H) = \mathrm{I}(\boldsymbol{s}; \boldsymbol{y}|\boldsymbol{H}{=}H) + \mathrm{I}(\boldsymbol{x}; \boldsymbol{y}|\boldsymbol{s}, \boldsymbol{H}{=}H), \tag{7}$$

where $\boldsymbol{x}$ is the noiseless received signal. Observing that $\boldsymbol{s}$, $\boldsymbol{x}$ and $\boldsymbol{y}$ form a Markov chain $\boldsymbol{s} \to \boldsymbol{x} \to \boldsymbol{y}$, the second term on the right-hand side of (6) vanishes, as $\boldsymbol{s}$ and $\boldsymbol{y}$ are independent given $\boldsymbol{x}$. The second term on the right-hand side of (7) can be written as

$$\begin{aligned}\mathrm{I}(\boldsymbol{x}; \boldsymbol{y}|\boldsymbol{s}, \boldsymbol{H}{=}H) &= \mathrm{h}(\boldsymbol{y}|\boldsymbol{s}, \boldsymbol{H}{=}H) - \mathrm{h}(\boldsymbol{y}|\boldsymbol{s}, \boldsymbol{x}, \boldsymbol{H}{=}H)\\ &= \mathrm{h}(\boldsymbol{y}|\boldsymbol{s}, \boldsymbol{x}, \boldsymbol{H}{=}H) - \mathrm{h}(\boldsymbol{y}|\boldsymbol{s}, \boldsymbol{x}, \boldsymbol{H}{=}H)\\ &= 0,\end{aligned} \tag{8}$$

since knowledge of $\boldsymbol{s}$ and $\boldsymbol{H}$ also implies knowledge of $\boldsymbol{x} = \boldsymbol{H}\boldsymbol{s}$, and thus, $\mathrm{h}(\boldsymbol{y}|\boldsymbol{s}, \boldsymbol{H} = H) = \mathrm{h}(\boldsymbol{y}|\boldsymbol{s}, \boldsymbol{x}, \boldsymbol{H} = H)$. Note that this argument does not require an invertible $\boldsymbol{H}$, and thus, (8) holds even when $\boldsymbol{H}$ is rank deficient. From (6), (7) and (8) we obtain

$$\mathrm{I}(\boldsymbol{s}; \boldsymbol{y}|\boldsymbol{H} = H) = \mathrm{I}(\boldsymbol{x}; \boldsymbol{y}|\boldsymbol{H} = H), \tag{9}$$

and the total mutual information from (5) reads as

$$\mathrm{I}(\boldsymbol{s}; \boldsymbol{y}, \boldsymbol{H}) = \mathrm{E}_{\boldsymbol{H}}[\mathrm{I}(\boldsymbol{x}; \boldsymbol{y}|\boldsymbol{H} = H)]. \tag{10}$$

Hence, it suffices to evaluate the conditional mutual information from $\boldsymbol{x}$ to $\boldsymbol{y}$. For notational simplicity we will drop the dependence on $\boldsymbol{H} = H$ from now on. The mutual information of interest (10), now written as $\mathrm{I}(\boldsymbol{x}; \boldsymbol{y})$, equals

$$\begin{aligned}\mathrm{I}(\boldsymbol{x}; \boldsymbol{y}) &= \mathrm{h}(\boldsymbol{y}) - \mathrm{h}(\boldsymbol{y}|\boldsymbol{x})\\ &= -\int \mathrm{p}(\boldsymbol{y})\log(\mathrm{p}(\boldsymbol{y}))\mathrm{d}\boldsymbol{y}\\ &\quad + \iint \mathrm{p}(\boldsymbol{x}, \boldsymbol{y})\log(\mathrm{p}(\boldsymbol{y}|\boldsymbol{x}))\mathrm{d}\boldsymbol{y}\mathrm{d}\boldsymbol{x}.\end{aligned} \tag{11}$$

Since the noise vector is i.i.d. and the nonlinear operator $g(\bullet)$ acts on each antenna separately, the conditional distribution of $\boldsymbol{y}$ given $\boldsymbol{x}$ can be split as

$$\mathrm{p}(\boldsymbol{y}|\boldsymbol{x}) = \prod_{i=1}^{N_{\mathrm{R}}}\mathrm{p}(y_i|x_i), \tag{12}$$

where $y_i$ and $x_i$ are the $i$-th elements of the vectors $\boldsymbol{y}$ and $\boldsymbol{x}$, respectively. The nonlinear operation on the received signal is described by

$$y_{i,\text{ampl.}} = g_{\text{ampl.}}(r_i) = \sqrt{\Re\{r_i\}^2 + \Im\{r_i\}^2}, \tag{13}$$

$$y_{i,\text{phase}} = g_{\text{phase}}(r_i) = \arg(r_i) = \tan^{-1}\left(\frac{\Im\{r_i\}}{\Re\{r_i\}}\right), \tag{14}$$

$i = 1, \ldots, N_{\mathrm{R}}$, for amplitude and phase detection, respectively. The inverse tangent in (14) takes into consideration the quadrant where $r_i$ lies in. When $\boldsymbol{x}$ is known, $\boldsymbol{r}$ is complex Gaussian distributed with $\mathcal{CN}(\boldsymbol{x}, \sigma_w^2\boldsymbol{I}_{N_{\mathrm{R}}})$. Its amplitude is Ricean distributed [7]

$$\mathrm{p}_{\text{ampl.}}(y_i|x_i) \;=\; \frac{2y_i}{\sigma_w^2}e^{-\frac{y_i^2+|x_i|^2}{\sigma_w^2}}I_0\left(\frac{2y_i|x_i|}{\sigma_w^2}\right), \tag{15}$$

while the distribution of the phase is given by Pawula [8]

$$\begin{aligned}\mathrm{p}_{\text{phase}}(\Delta\phi_i|x_i) &= \frac{e^{-\rho_i}}{\sigma_w^2} + \sqrt{\frac{\rho_i}{4\pi}}e^{-\rho_i\sin^2\Delta\phi_i}\\ &\quad\cdot\cos\Delta\phi_i\,\mathrm{erfc}(-\sqrt{\rho_i}\cos\Delta\phi_i),\end{aligned} \tag{16}$$

where $\rho_i = |x_i|^2/\sigma_w^2$ and $\Delta\phi_i = y_{i,\text{phase}} - \arg(x_i) \in [0, 2\pi)$. $I_0(\bullet)$ is the zeroth order modified Bessel function of the first kind and erfc$(\bullet)$ is the complementary error function.

The capacity of the MIMO channel with nonlinear detection is the maximum of (10) over all input distributions

$$C = \underset{\mathrm{p}(\boldsymbol{x})}{\operatorname{argmax}} \, \mathrm{E}_{\boldsymbol{H}}[\mathrm{I}(\boldsymbol{x};\boldsymbol{y}|\boldsymbol{H}=H)]. \tag{17}$$

Since the analytical solution of (17) is intractable, we compute the achievable rates for two input distributions, namely for a constant amplitude uniform-phase, and for a circularly symmetric complex Gaussian distribution. The latter distribution is of special interest since it achieves capacity for linear detection [1].

## IV. Numerical Computation

The integrals in (11) are computed using *Monte Carlo* (MC) integration. MC methods are especially important for the computation of multi-dimensional integrals, i.e., more than 4 dimensions, where the traditional numerical methods become computationally prohibitive. Due to (12), (15), (16), the distribution $\mathrm{p}(\boldsymbol{y}|\boldsymbol{x})$ appearing in the second integral of (11) is known analytically for both amplitude and phase detection. The MC estimate of the conditional entropy $\mathrm{h}(\boldsymbol{y}|\boldsymbol{x})$ is given by

$$\mathrm{h}(\boldsymbol{y}|\boldsymbol{x}) \simeq -\frac{1}{N}\sum_{i=1}^{N} \log(\mathrm{p}(\boldsymbol{y}_i|\boldsymbol{x}_i)), \tag{18}$$

where $\boldsymbol{x}_i$ and $\boldsymbol{y}_i$ are samples generated according to the joint distribution $\mathrm{p}(\boldsymbol{x},\boldsymbol{y})$. The distribution of $\boldsymbol{y}$ is necessary for the computation of $\mathrm{h}(\boldsymbol{y})$. However, $\mathrm{p}(\boldsymbol{y})$ is generally not known. For a Gaussian input alphabet $\boldsymbol{s}$, $\boldsymbol{r} = \boldsymbol{H}\boldsymbol{s} + \boldsymbol{w}$ is Gaussian with $\boldsymbol{s} \sim \mathcal{CN}(\sigma_s^2 \boldsymbol{H}\boldsymbol{H}^{\mathrm{H}} + \sigma_w^2 \boldsymbol{I})$. Closed form expressions of $\mathrm{p}(\boldsymbol{y}) = \mathrm{p}(g(\boldsymbol{r}))$ exist only for specific values of $N_{\mathrm{R}}$. In a system with a single receive antenna, $N_{\mathrm{R}} = 1$, $y$ is uniformly distributed in $[0, 2\pi)$ for phase detection, and Rayleigh distributed for amplitude detection [7]. For $N_{\mathrm{R}} = 2$, the amplitude and phase distributions are given by [9], [10]

$$\mathrm{p}_{\text{ampl.}}(\boldsymbol{y}) = 4y_1y_2 \det(\boldsymbol{\Phi}) e^{-(\boldsymbol{\Phi}_{11}y_1^2 + \boldsymbol{\Phi}_{22}y_2^2)} I_0(2|\boldsymbol{\Phi}_{12}|y_1y_2), \tag{19}$$

$$\mathrm{p}_{\text{phase}}(\boldsymbol{y}) = \frac{\det(\boldsymbol{\Phi})}{8\pi^2 \boldsymbol{\Phi}_{11}\boldsymbol{\Phi}_{22}} \left[\frac{1}{1-\lambda^2} - \frac{\lambda \cos^{-1}\lambda}{(1-\lambda^2)^{3/2}}\right], \tag{20}$$

where $\boldsymbol{\Phi} = (\mathrm{E}[\boldsymbol{r}\boldsymbol{r}^{\mathrm{H}}])^{-1} = (\sigma_s^2 \boldsymbol{H}\boldsymbol{H}^{\mathrm{H}} + \sigma_w^2 \boldsymbol{I})^{-1}$,

$$\lambda = \frac{\boldsymbol{\Phi}_{12}}{\sqrt{\boldsymbol{\Phi}_{11}\boldsymbol{\Phi}_{22}}} \cos(y_1 - y_2 - \chi_{12}), \tag{21}$$

and $\chi_{ij} = \arg(\boldsymbol{\Phi}_{ij})$. The amplitude distribution for $N_{\mathrm{R}} = 3$ is given by [9], [11]

$$\begin{aligned}\mathrm{p}(\boldsymbol{y}) \;=\; & 8y_1y_2y_3 \det(\boldsymbol{\Phi}) e^{-(\boldsymbol{\Phi}_{11}y_1^2 + \boldsymbol{\Phi}_{22}y_2^2 + \boldsymbol{\Phi}_{33}y_3^2)} \cdot \\ & \sum_{m=0}^{\infty} [\varepsilon_m (-1)^m I_m(2|\boldsymbol{\Phi}_{12}|y_1y_2) I_m(2|\boldsymbol{\Phi}_{23}|y_2y_3) \cdot \\ & I_m(2|\boldsymbol{\Phi}_{31}|y_3y_1) \cos(m(\chi_{12} + \chi_{23} + \chi_{31}))], \end{aligned} \tag{22}$$

where $\varepsilon_m$ is the Neumann constant ($\varepsilon_0 = 1$, $\varepsilon_m = 2$ for $m > 1$). No closed form expression exists for the trivariate phase distribution. For $N_{\mathrm{R}} > 3$[†], we use MC integration to estimate the probability density of certain realizations $\boldsymbol{y}_i$

$$\mathrm{p}(\boldsymbol{y}_i) \;=\; \int \mathrm{p}(\boldsymbol{x})\,\mathrm{p}(\boldsymbol{y}_i|\boldsymbol{x})\mathrm{d}\boldsymbol{x} \simeq \frac{1}{M}\sum_{j=1}^{M} \mathrm{p}(\boldsymbol{y}_i|\boldsymbol{x}_j). \tag{23}$$

The samples $\boldsymbol{x}_j$ are generated according to the distribution $\mathrm{p}(\boldsymbol{x})$. The MC estimate of the entropy of $\boldsymbol{y}$ is finally given by

$$\mathrm{h}(\boldsymbol{y}) \simeq -\frac{1}{N}\sum_{i=1}^{N} \log(\mathrm{p}(\boldsymbol{y}_i)), \tag{24}$$

where $\boldsymbol{y}_i$ are realizations of $\boldsymbol{y}$, with probability density $\mathrm{p}(\boldsymbol{y}_i)$, computed by (19), (20), (22), or (23), depending on $N_{\mathrm{R}}$. Note that the estimate in (23) becomes unreliable for high SNR, since the conditional pdf becomes very narrow. Selecting an appropriate auxiliary function and using importance sampling is a means to improve the numerical accuracy [12].

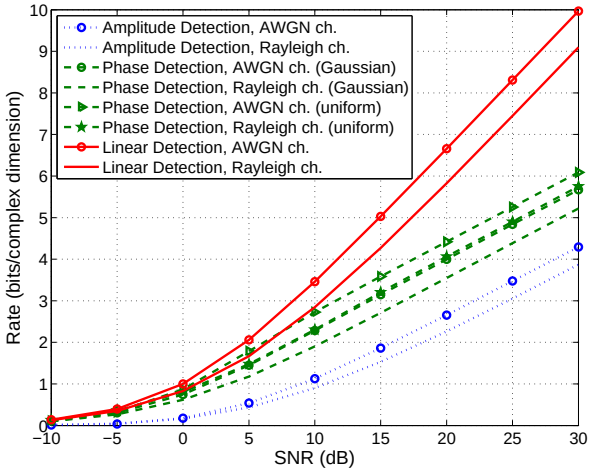


Fig. 2. SISO system.

## V. Simulation Results

In the following plots, solid, dotted and dashed lines stand for linear, amplitude and phase detection, respectively. The solid curves are evaluated using the capacity equation (2), while the dashed and dotted curves refer to numerically computed achievable rates. The input distribution of the nonlinear detection rates is circularly symmetric complex Gaussian, unless stated otherwise. The SNR is defined in (3). The channel matrix has i.i.d. zero-mean unit-variance circularly symmetric Gaussian entries.

### A. Ergodic Rates

We assume a fast fading channel and explore the ergodic achievable rates. Fig. 2 depicts the rates for a SISO system ($N_{\mathrm{T}} = N_{\mathrm{R}} = 1$), both for an AWGN channel and for Rayleigh fading. We observe that linear detection is superior to both

[†]An infinite sum expression exists for the quadrivariate case when $\chi_{14} = \chi_{41} = 0$ [11], but this in not relevant in our scenario.

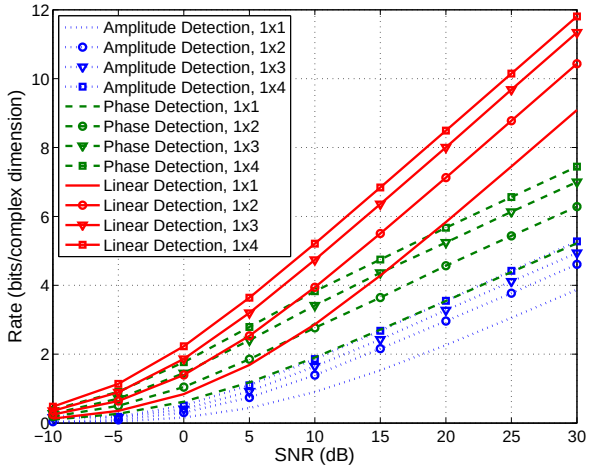


Fig. 3. SIMO system.

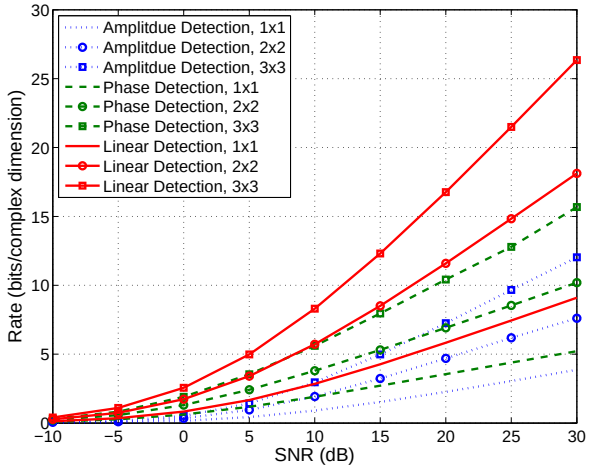


Fig. 4. MIMO system, $N_{\mathrm{T}} = N_{\mathrm{R}}$.

nonlinear techniques. Furthermore, the slope of the rate curve for nonlinear detection at high SNR is approximately half the slope of linear detection, and thus, equal to the slope of linear detection using one-dimensional (real-valued) signals. We also plot the capacity for phase detection, which is achieved when the input signal has unit amplitude and uniform phase [5]. The uniform distribution is capacity achieving only in the SISO case. For higher number of receive antennas, simulations show that the uniform distribution yields the same rates as the complex Gaussian distribution. This effect rises from the MIMO channel multiplexing. As a matter of fact, the distribution of $\boldsymbol{x}$ is close to a Gaussian and depends less and less on the distribution of $\boldsymbol{s}$. Hence, in the rest of the paper we use only the complex Gaussian input distribution. Finally, phase detection outperforms amplitude detection at all SNR. This property holds for all combinations of $N_{\mathrm{T}}$ and $N_{\mathrm{R}}$.

The rate gain for a *multiple input single output* (MISO) systems ($N_{\mathrm{R}} = 1$) is negligible, since the transmitter does not exploit CSI. In the contrary, we obtain an array gain for *single input multiple output* (SIMO) systems ($N_{\mathrm{T}} = 1$). Fig. 3 depicts the respective rates. We observe that the use of more receive antennas continuously improves the achievable rates. The nonlinear techniques behave in the same way as linear detection. The array gain is higher at the introduction of the second antenna, and becomes smaller thereafter, since the rate scales with the logarithm of the SNR. Like in the MISO case, increasing the number of receive antennas does not influence the slope of the nonlinear rate curves.

Fig. 4 depicts a MIMO system with $N_{\mathrm{T}} = N_{\mathrm{R}}$. As expected, the slope of the nonlinear rate curves increases when increasing the number of transmit and receive antennas. Furthermore, the slope of the nonlinear rates remains approximately half the slope of the respective linear capacity, like in the SISO case. For example, for $N_{\mathrm{T}} = N_{\mathrm{R}} = 2$, the slope of amplitude and phase detection at high SNR is the same as the slope of linear detection with $N_{\mathrm{T}} = N_{\mathrm{R}} = 1$.

Fig. 5a compares a system with $N_{\mathrm{T}} = 2$ and variable number of receive antennas $N_{\mathrm{R}} = 1, \ldots, 4$. For linear detection, the slope of the capacity curves for $N_{\mathrm{R}} \geq 2$ remains the same, since the degrees of freedom $N_{\min} = 2$ are unchanged and fully exploited. The parallel shift is the result of a power gain. However, this is not true for the nonlinear techniques. Their slope continues to increase as we add more receive antennas, but always remains lower than the linear detection slope. We approximate the rate curves with $R = \alpha \log_2(1 + \beta \mathrm{SNR})$ and plot twice the estimated spatial multiplexing gain $\alpha$ in Fig. 5b. We observe how the nonlinear detectors exploit the additional receive antennas to achieve higher spatial multiplexing gains. However, they miss one real degree of freedom, i.e., they reach a spatial multiplexing gain up to $2N_{\min} - 1 = 3$ in real dimensions. We justify our observation by means of an example. In an $N_{\mathrm{T}} = 2$, $N_{\mathrm{R}} = 2$ system the received signal consists of two phases and two amplitudes. A phase detector

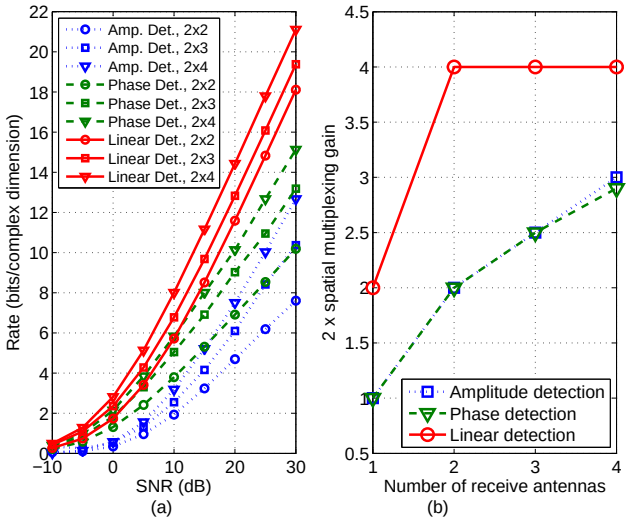


Fig. 5. MIMO system, $N_{\mathrm{T}} = 2$ and varying $N_{\mathrm{R}}$. (a) Achievable rates and (b) spatial multiplexing gain in real-valued dimensions.

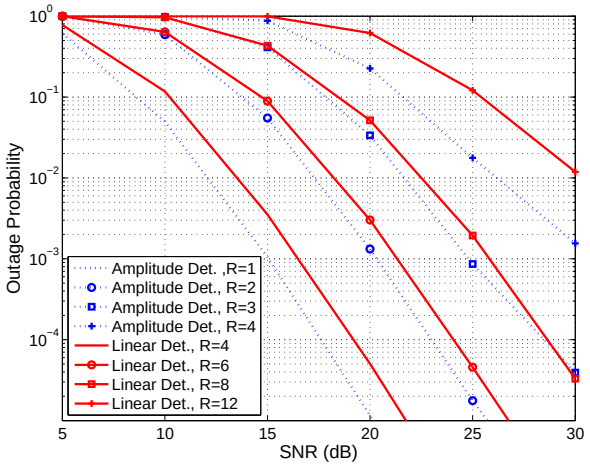


Fig. 6. Outage probabilities for different outage rates, amplitude and linear detection. $N_{\mathrm{T}} = N_{\mathrm{R}} = 2$.

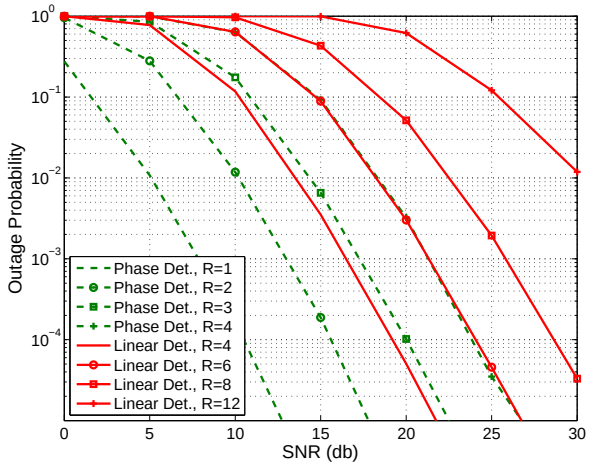


Fig. 7. Outage probabilities for different outage rates, phase and linear detection. $N_{\mathrm{T}} = N_{\mathrm{R}} = 2$.

extracts the two phases of the signal, but has no information about the two amplitudes. However, if $N_{\mathrm{R}} = 3$, we can deduce an equation relating the two amplitudes by combining the three observed phases. Thus, we only miss one more equation in order to also extract the two amplitudes. Nevertheless, there will always remain an ambiguity regarding the amplitudes, since multiplying the complex-valued received vector by a scalar would change the amplitudes but not the phases.

### *B. Outage Probability and Diversity*

We assume a slow fading scenario, where averaging over different channel realizations is not possible. The outage probability is non-zero for any given outage rate. We consider a $N_{\mathrm{T}} = N_{\mathrm{R}} = 2$ system and investigate the outage probability for different outage rates. The slope of the outage probability curves at high SNR reflects the diversity that is achieved at a given outage rate. It is known that the maximum diversity with linear detection is $N_{\mathrm{T}}N_{\mathrm{R}}$ [6]. However, it is not clear whether nonlinear detection achieves the same maximum diversity.

Fig. 6 depicts the outage probability curves for amplitude and linear detection. The leftmost curves drop four orders of magnitude within a range of 10 dB's, which shows that amplitude detection also achieves the maximum diversity of the MIMO channel. The same holds for phase detection, as illustrated in Fig. 7. We also observe that the slope of the outage probability curves flattens for larger outage rates. This is due to transition toward other operating regions on the diversity-multiplexing tradeoff plane, as explained in [13]. These results hint that nonlinear detection, like linear detection, exploits the full MIMO diversity.

## VI. Conclusions

We investigated achievable rates of MIMO systems with nonlinear detection and perfect CSI at the receiver. Although the performance is inferior to linear detection, the nonlinear techniques unexpectedly exploit additional receive antennas to achieve higher spatial multiplexing gains. This is a promising result, since it may be cheaper to use more nonlinear receiver chains than linear ones. Consequently, nonlinear MIMO receivers provide an interesting low-cost/low-power solution for cheap nodes in distributed systems like sensor networks. Furthermore, nonlinear detection fully exploits the diversity of the MIMO channel, as revealed by the outage probability behavior.

## References

[1] I. E. Telatar, "Capacity of Multi-antenna Gaussian Channels," in *European Transactions on Telecommunications*, November 1999, pp. 585–595.

[2] G. J. Foschini and M. J. Gans, "On Limits of Wireless Communications in a Fading Environment when Using Multiple Antennas," in *Wireless Personal Communications*, vol. 6, no. 3, March 1998, pp. 311–355.

[3] S. Cui, A. J. Goldsmith, and A. Bahai, "Energy-efficiency of MIMO and Cooperative MIMO Techniques in Sensor Networks," *IEEE Journal on Selected Areas in Communications*, vol. 22, pp. 1089–1098, August 2004.

[4] F. Althaus, *A New Low-Cost Approach to Wireless Communication over Severe Multipath Fading Channels*. Logos Verlag Berlin, 2002.

[5] J. P. Aldis and A. G. Burr, "The Channel Capacity of Discrete Time Phase Modulation in AWGN," *IEEE Transactions on Information Theory*, vol. 39, pp. 184–185, January 1993.

[6] D. Tse and P. Viswanath, *Fundamentals of Wireless Communications*. Cambridge University Press, 2005.

[7] A. Papoulis, *Probability, Random Variables, and Stochastic Processes*, 3rd ed. McGraw-Hill, 1991.

[8] R. Pawula, S. Rice, and J. Roberts, "Distribution of the Phase Between Two Vectors Perturbed by Gaussian Noise," *IEEE Transactions on Communications*, vol. 30, pp. 1828–1841, August 1982.

[9] K. S. Miller, *Multidimensional Gaussian Distributions*. Wiley, 1964.

[10] R. K. Mallik, "On Multivariate Rayleigh and Exponential Distributions," in *IEEE Transactions on Information Theory*, vol. 49, no. 6, June 2003, pp. 1499–1515.

[11] Y. Chen and C. Tellambura, "Infinite Series Representaion of the Trivariate and Quadrivariate Rayleigh Distribution and Their Applications," *IEEE Transactions on Communications*, vol. 53, pp. 2092–2101, December 2005.

[12] D. J. C. MacKay, "Introduction to Monte Carlo methods," in *Learning in Graphical Models*. Kluwer Academic Press, 1998, pp. 175–204.

[13] K. Azarian and H. El Gamal, "On the Utility of a 3 db SNR Gain in MIMO Channels," in *IEEE International Symposium on Information Theory*, July 2006, pp. 2274–2278.